J. Phys. B: At. Mol. Opt. Phys. **32** (1999) L73–L79. Printed in the UK PII: S0953-4075(99)99593-7

LETTER TO THE EDITOR

Differential cross sections in antiproton– and proton–helium collisions

Kh Khayyat†, T Weber†, R Dörner†, M Achler†, V Mergel†, L Spielberger†, O Jagutzki†, U Meyer‡, J Ullrich§, R Moshammer§, W Schmitt‡, H Knudsen‖, U Mikkelsen‖, P Aggerholm‖, E Uggerhoej¶, S P Moeller¶, V D Rodríguez[+], S F C O'Rourke[*], R E Olson[#], P D Fainstein[•], J H McGuire†[○] and H Schmidt-Böcking†

† Institut für Kernphysik, August-Euler-Straße 6, D60486 Frankfurt am Main, Germany
‡ Gesellschaft für Schwerionenforschung, D64291 Darmstadt, Germany
§ Universität Freiburg, Fakultät für Physik, Hermann-Herderstraße 3, D79104 Freiburg, Germany
‖ Institute of Physics and Astronomy, University of Aarhus, DK8000 Aarhus C, Denmark
¶ Institute of Storage Ring Facilities, University of Aarhus, DK8000 Aarhus C, Denmark
[+] Universidad de Buenos Aires, Departamento de Física, 1428 Buenos Aires, Argentina
[*] The Queen's University of Belfast, School of Mathematics and Physics, Belfast BT7 1NN, UK
[#] University of Missouri, Rolla, MO 65401, USA
[•] Centro Atómico Bariloche, 8400 S C de Bariloche, Argentina
[○] Tulane University, New Orleans, LA 70118, USA

Received 24 November 1998, in final form 13 January 1999

Abstract. Cross sections are presented for the first time for antiproton–helium collisions at an energy of 945 keV differential in longitudinal electron and recoil-ion momenta. The longitudinal momentum distributions for antiproton impact are compared with 1 MeV proton–helium collision. The electron and the recoil-ion momentum distributions for antiprotons agree with those for protons to within 10%. We did not observe a difference between antiproton impact and proton impact. A comparison with CDW and CTMC theories is presented.

In collisions of charged particles with atoms effects of projectile charge asymmetries have been observed in total cross sections for ionization of atoms [1]. For example, in single ionization these asymmetries give rise to the Barkas effect in energy deposition in solids [2]. Differences in single ionization of helium have been observed [3] to be greater than 10% at energies below 500 keV. Projectile charge asymmetries in double ionization of helium occur for incident protons and antiprotons at energies below 10 MeV, and are thought to be caused by dynamical electron correlation [4–21] (for a review see [22]). However, until now no observation has been made of differential cross sections using antiprotons.

In this paper we report observations of cross sections for single ionization of helium differential in the longitudinal momentum of ions and electrons for both protons and antiprotons at energies near 1 MeV. In principle, differential observations give more specific information about the nature of projectile charge asymmetries than do total cross sections where only average information is obtained. At 1 MeV both classical trajectory Monte Carlo (CTMC) [13, 23, 37] and quantum mechanical continuum distorted-wave (CDW) [24–30] calculations performed by us predict differences in the longitudinal momentum

spectrum of 10% or more for ionization by protons and antiprotons. These differences may be interpreted as being due to differences in post-collision interactions (PCI) of the projectile with the continuum electron, i.e. charge asymmetries in the final state continuum wavefunction.

In our measurements we applied the technique of cold-target recoil-ion momentum spectroscopy (COLTRIMS) (see [33] for a recent review) to detect the emitted recoil ions and electrons in the 945 keV antiproton–helium single-ionization process. Furthermore, the same differential cross sections for the 1 MeV proton–helium system were measured and are compared with antiproton results.

Using the experimental technique of COLTRIMS, the antiproton–helium experiment was carried out at the low-energy antiproton ring (LEAR) at CERN. The LEAR antiproton beam had an intensity of the order of 10^6 $\bar{\mathrm{p}}/\mathrm{s}$ at a minimum energy of 5.9 MeV and was degraded to 945 keV. The goal of the experiment was to investigate the single ionization of helium at the lowest possible energy for the antiproton beam. Since the use of a foil degrader enlarges the beam diameter, which reduces the desired resolution, one had to make a compromise between the beam diameter and energy. A mylar foil of thickness 133 μm combined with a 200 μm thick polyvinyltoluene scintillator were used to degrade the energy of the antiprotons to about 945 keV. A time-of-flight measurement between the signals of the scintillator and the projectile detector, which was placed downstream of the gas target, was used to determine the projectile energy distribution and to detect the coincidence with the emitted recoil ion and electron and thus measure their time of flight. After degradation, the diameter of the antiproton beam was about 6 mm (FWHM) at the intersection zone with the He gas jet.

The 1 MeV proton experiment was performed at the Van de Graaf accelerator of the University of Frankfurt. To measure the time of flight of the recoil ion and the electron, the proton beam was pulsed with a rate of 2 MHz and a time resolution of 1.5 ns. The proton beam diameter was about 0.5 mm.

Figure 1 shows the schematics of the COLTRIMS system used. It is able to measure the recoil ions with a solid angle of 4π, while the electron detection solid angle depends on the applied potential on the spectrometer. Using a supersonic gas jet device the COLTRIMS apparatus produces a target density of 1×10^{11} atom/cm^2 for a target diameter of 1 mm and an internal temperature of 0.1 K in the direction of jet expansion. In the spectrometer the recoil ions produced are extracted by a homogenous electric field created between two parallel meshes with potentials U_1 and U_4. An electrostatic lens with a potential of $|U_2 - U_3|$ in the extraction field focuses the recoil ions after their drift through a field-free region onto the position-sensitive detector to eliminate the influence of the target extension on the momentum resolution. Towards the opposite side the electrons are detected with a position-sensitive detector. The electric field was so strong that it could detect electrons with longitudinal momentum up to 1 au (perpendicular to the electric field) in the case of antiproton collisions and 1.2 au for protons. Two different spectrometer potentials $\Delta U = U_1 - U_2$ (which are divided on a 7 cm extraction field region) should be considered in order to detect more electrons by high ΔU and to obtain better recoil-ion momentum resolution by low ΔU. But because of the limited scheduled beam time at LEAR we were able to take data only for one spectrometer potential, 300 V, in the antiproton case, while in the case of protons we have performed measurements of electrons at 500 V and of the recoil ions at 50 V. In addition, the huge divergence of the antiproton beam allowed us to focus the recoil ions only in the longitudinal direction, which means that transverse momentum could not be measured in the case of antiproton impact. More details about the set-up can be found in [31–33, 35].

The times of flight for the electrons and recoil ions were measured to determine one component of the transversal momentum distribution (x-direction). The longitudinal

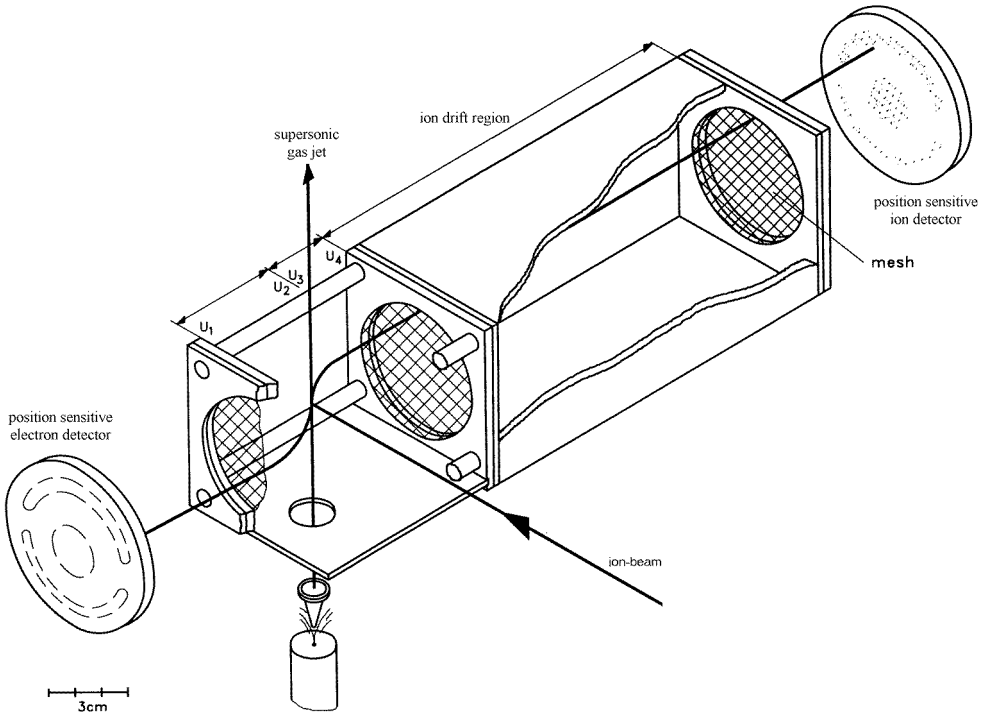

Figure 1. Schematic diagram of COLTRIMS with the jet, spectrometer and the position-sensitive channel-plate detector (PSCD).

momentum (z-direction) was determined from the position of the recoil ion and the electron on the position-sensitive detectors. The main components of the detector are Z-stack multichannel plates and a wedge and strip anode.

Figure 2(*a*) shows the experimental data of the emitted electrons for antiproton impact. The data were normalized with respect to the total cross section of Andersen *et al* [34]. Surprisingly these data show that the electrons move slightly in the forward direction with a peak position at $+0.087 \pm 0.039$ au. The CTMC predicts more emission to negative momentum values. The data for recoil ions in figure 2(*b*) disagree with CTMC, whereas CDW agrees within the experimental error. The CTMC predicts a more forward emission than CDW. Although the CDW curve shows a symmetric distribution around zero momentum, the data in figure 2(*b*) show a slight peak position shift of the recoil ions in the forward direction.

In figure 3 the CDW underestimates the cross sections of both electrons and recoil ions in the case of proton–helium collisions. Although figure 3(*a*) shows that both theories predict forward emission of the electrons, the experimental peak position ($+0.075 \pm 0.007$ au) shows somewhat better agreement with CTMC than CDW. Figure 3(*b*) shows that the recoil ions have almost a symmetric distribution about zero momentum, which means that the recoil ion in this interaction behaves as a spectator during the collision process. In contrast to our experimental data, CDW predicts a small backward shift of the peak. In figure 3(*b*) CTMC shows a nearly symmetric distribution around zero momentum in agreement with the experimental data. The experimental data in the work of Dörner *et al* [35] for proton–helium collisions by 1 MeV agree very well with ours. Dörner *et al* have also measured the recoil ions in the longitudinal direction and have found that the recoil ions are only spectators in the collision process.

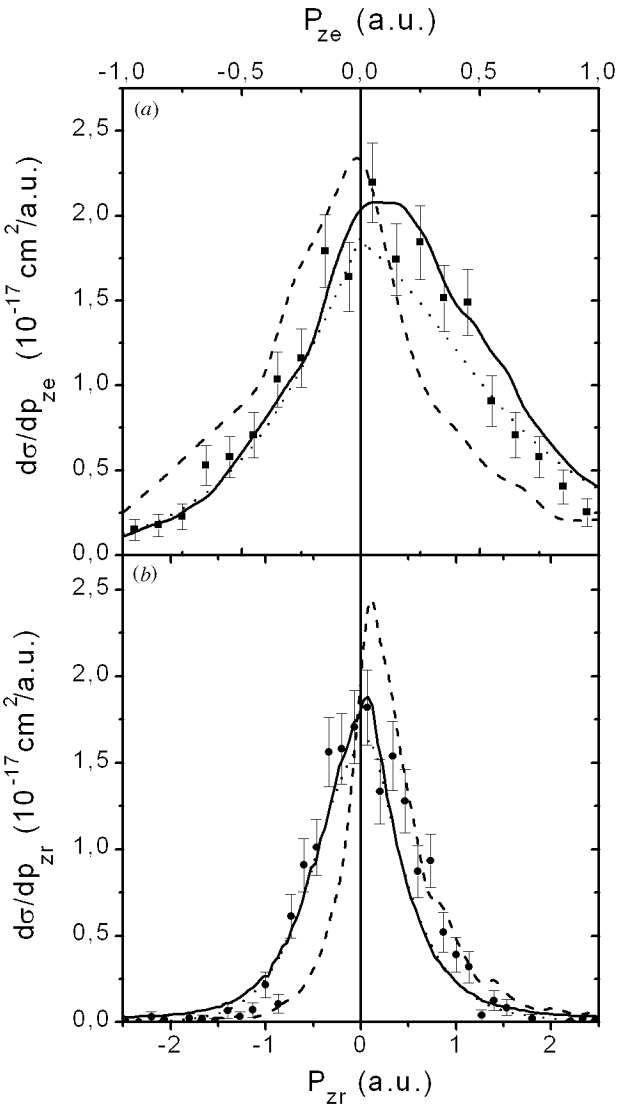

Figure 2. Longitudinal momentum distribution for single ionization of helium by 945 keV antiproton (data points) in comparison with proton collision (full curve). (*a*) Electron momentum data; (*b*) recoil-ion data. The theoretical calculations represent antiproton collision: dotted curve, CDW result; broken curve, CTMC result.

If the data for antiprotons and protons are compared (see figure 2) we find that both momentum distributions are almost the same, except that the peak position of electrons for proton impact is slightly shifted in the forward direction.

The predictions that the recoil ions move backwards and the electrons move forwards after the collision by a positive projectile and the opposite by a negative projectile [25, 36, 37], are not fulfilled in the energy regime of this experiment. The data show that at our projectile energy the sign of the projectile has a negligible effect on the emitted electron or recoil-ion distributions after the collision. This indicates that PCI effects which depend on the sign of

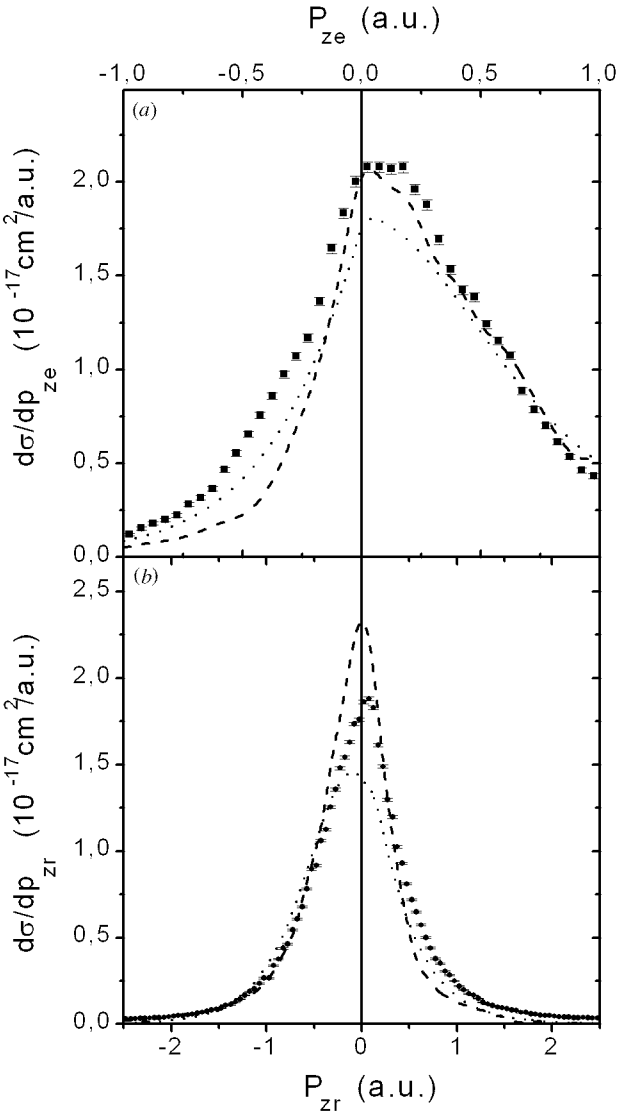

Figure 3. Longitudinal momentum distribution for single ionization of helium by 1 MeV protons (data points) in comparison with theory: CTMC (broken curve) and CDW (dotted curve).

the projectile charge are very small in our collisions with fast, low-Z projectiles. This differs somewhat from the findings of Moshammer *et al* [36] for highly charged ions colliding with matter, where the dependence on the long-range effect of the projectile Coulomb potential is very strong in the Ni^{24+}–helium collision. In their work Moshammer *et al* have also introduced CTMC calculations for an imaginary anti-nickel ($\overline{Ni}^{24-}$)–helium collision and stated that the data are a mirror image of the Ni^{24+}–helium collision.

Fainstein predicts [25] that if one extrapolates the peak position of the CDW curve from low to high projectile energies, then the longitudinal electron momentum p_{ze} converges to 0 au due to the dominance of dipole transitions. CDW predicts that in both cases (antiprotons and

protons) p_{ze} would converge to zero value at high energies, but faster in the case of antiprotons. In our high-velocity experiment the peak positions are found at about the same positive value for both cases, but not at zero as CDW predicts.

In conclusion, COLTRIMS has been used to compare the longitudinal momentum differential cross sections for electrons and recoil ions in antiproton– and proton–helium single ionization. It was found at about 1 MeV collision energy that for these collisions projectile charge asymmetries (e.g. PCI effects) are less than 10%. The data show that the recoil ions behave primarily as spectators and that the electron is the particle which compensates the projectile momentum loss, which is different from the results of previous experiments on highly charged ion collisions where the electron and the recoil ion compensate each others momenta. The data indicate that the electron peak positions for proton and antiproton collisions converge to the same value, which shows that the sign of the low-Z projectile does not play a major role in the collision dynamics above 1 MeV. Experimentally it remains a challenge to observe projectile charge asymmetries at low antiproton energies where this effect is expected to play a major role in the collision process.

KhK is grateful to the DAAD for financial support. RD and JMcG thank the Alexander von Humboldt Stiftung. HK would like to thank the Danish Natural Science Research Council for financial support. VM thanks the Studienstiftung des deutschen Volkes. The BMBF, GSI, the Graduiertenförderung des Landes Hessen, Willkomm-Stiftung, USDOE and DFG within the SFB 276 (project B8) are gratefully acknowledged for their financial support. We would like to thank the staff of CERN and IKF for the experiment installation and beam time.

References

[1] Christenson J H, Cronin J W, Fitch V L and Turlay R 1964 *Phys. Rev. Lett.* **13** 138
[2] Moeller S P *et al* 1997 *Phys. Rev.* A **56** 2930
[3] Hvelplund P *et al* 1994 *J. Phys. B: At. Mol. Opt. Phys.* **27** 925
[4] Andersen L H *et al* 1986 *Phys. Rev. Lett.* **57** 2147
[5] Andersen L H *et al* 1987 *Phys. Rev.* A **36** 3612
[6] McGuire J H 1997 *Electron Correlation Dynamics in Atomic Collisions* (Cambridge: Cambridge University Press)
[7] Ford A L and Reading J F 1994 *J. Phys. B: At. Mol. Opt. Phys.* **27** 4215
[8] Fang X and Reading J F 1991 *Nucl. Instrum. Methods* B **53** 453
[9] Ford A L and Reading J F 1988 *J. Phys. B: At. Mol. Opt. Phys.* **21** L685
[10] Ford A L and Reading J F 1990 *J. Phys. B: At. Mol. Opt. Phys.* **23** 2567
[11] McGuire J H 1982 *Phys. Rev. Lett.* **49** 1153
[12] McGuire J H 1992 *Adv. At. Mol. Opt.* **29** 219
[13] Meng L *et al* 1993 *J. Phys. B: At. Mol. Opt. Phys.* **26** 3387
[14] Reading J F and Ford A L 1987 *J. Phys. B: At. Mol. Phys.* **20** 3747
[15] Reading J F and Ford A L 1990 *Comment. At. Mol. Opt.* **23** 301
[16] Reading J F *et al* 1984 *Electronic and Atomic Collisions* ed J Eichler, I V Hertel and N Stolterfoht (Amsterdam: Elsevier) pp 201–11
[17] Ford A L and Reading J F 1985 *Nucl. Instrum. Methods* B **10/11** 12
[18] Ford A L and Reading J F 1991 *Nucl. Instrum. Methods* B **56/57** 196
[19] Olson R E *et al* 1989 *Phys. Rev.* A **40** 2843
[20] Reading J F and Ford A L 1987 *Phys. Rev. Lett.* **58** 543
[21] Reading J F, Ford A L and Fang X 1989 *Phys. Rev. Lett.* **62** 245
[22] Knudsen H and Reading J F 1992 *Phys. Rev. Rep.* **212** 107
[23] Olson R E 1993 *6th Int. Conf. on the Physics of Highly Charged Ions* vol 279, p 229
[24] Crothers D S F 1996 *Atomic, Molecular and Optical Physics Reference Book* (New York: AIP) ch 43
[25] Fainstein P D 1996 *J. Phys. B: At. Mol. Opt. Phys.* **29** L763
[26] O'Rourke S F C and Crothers D S F 1997 *J. Phys. B: At. Mol. Opt. Phys.* **30** 2443
[27] Crothers D S F and McCann J F 1983 *J. Phys. B: At. Mol. Phys.* **16** 3229

[28] Fainstein P D, Ponce V H and Rivarola R D 1991 *J. Phys. B: At. Mol. Opt. Phys.* **24** 3091
[29] Rodriguez V D, Wang Y D and Lin C D 1995 *Phys. Rev.* A **52** R9
[30] Fukuda H, Shimamura I, Vegh L and Watanabe T 1991 *Phys. Rev.* A **44** 1565
[31] Dörner R *et al* 1997 *Nucl. Instrum. Methods* B **124** 225
[32] Mergel V *et al* 1995 *Phys. Rev. Lett.* **74** 2200
[33] Ullrich J *et al* 1997 *J. Phys. B: At. Mol. Opt. Phys.* **30** 2917
[34] Andersen L H *et al* 1990 *Phys. Rev.* A **41** 6536
[35] Dörner R *et al* 1995 *J. Phys. B: At. Mol. Opt. Phys.* **28** 435
[36] Moshammer R *et al* 1994 *Phys. Rev. Lett.* **73** 3371
[37] Wood C J and Olson R E 1996 *J. Phys. B: At. Mol. Opt. Phys.* **29** L257